

# Molecular Docking Studies of some Antiviral and Antimalarial Drugs *Via* Bindings to 3CL-Protease and Polymerase Enzymes of the Novel Coronavirus (SARS-CoV-2)

Najim A. Al-Masoudi <sup>1,\*</sup> , Rita S. Elias <sup>2</sup>, Bahjat Saeed <sup>3</sup>

<sup>1</sup> Department of Chemistry, College of Science, University of Basrah, Basrah, Iraq. Present address: Constance, Germany

<sup>2</sup> Department of Pharmaceutical Chemistry, College of Pharmacy, University of Basrah, Basrah, Iraq

<sup>3</sup> Department of Chemistry, College of Education of Pure Science, University of Basrah, Basrah, Iraq

\* Correspondence: najim.al-masoudi@gmx.de;

Scopus Author ID 7003637680

Received: 11.04.2020; Revised: 7.05.2020; Accepted: 9.05.2020; Published: 13.05.2020

**Abstract:** The rapid spread of the novel coronavirus (SARS-CoV-2) as a serious threat to the world public health is in dire need of finding potential therapeutic agents. Chinese have tested several antiviral and antimalarial drugs as potent inhibitors for the novel virus, such as remdesivir, chloroquine, hydroxychloroquine, umifenovir and favipiravir. In this study, we used the molecular docking models to study the binding interactions between these pharmaceuticals, as well as our proposed remdesivir analogue (AZCV-20) with the 3CLpro and RNA-dependent RNA polymerase (RdRp) of the SARS-CoV-2, using MEO and Autodock4 methods. Our study provides insight into the possible role of structural flexibility and efficacy during interactions between 3CLpro, RdRp and the drugs.

**Keywords:** Antiviral and antimalarial drugs; Molecular Docking; SARS-CoV-2; 3CLpro; RNA-dependent RNA polymerase (RdRp).

© 2020 by the authors. This article is an open access article distributed under the terms and conditions of the Creative Commons Attribution (CC BY) license (<https://creativecommons.org/licenses/by/4.0/>).

## 1. Introduction

A novel severe acute respiratory syndrome coronavirus (SARS-CoV-2) was identified from respiratory illness patients in Wuhan, China in December 2019 [1, 2], which is closely related to severe acute respiratory syndrome CoV (SARS-CoV). Today, no specific drugs are available to treat this disease. Thus, there remains an urgent need for the development of specific antiviral therapeutics toward SARS-CoV-2. A number of pharmaceuticals already being tested [3-5], but a better understanding of the underlying pathobiology is required. Due to the similarities of SARS-CoV-2 with the original SARS-CoV, several laboratories are focusing on the viral genome structural proteins like spike glycoprotein (S), a small envelope protein (E), matrix glycoprotein (M), nucleocapsid protein (N) [6, 7], the 3CLpro, the main protease required for the maturation of coronaviruses, the protease polymerase (RdRp) is vital for the viral life cycle, making it an attractive target of anti-coronavirus drug development.

Drugs like ribavirin, interferon-alpha, lopinavir-ritonavir (kaletra), required for the maturation of coronaviruses (3CLpro) [8, 9] and the RNA-dependent RNA umifenovir, favipiravir, emtricitabine/tenofovir alafenamide, corticosteroids, and cyclophilin have been tested in patients with SARS or MERS, although the efficacy of some drugs remains controversial [10], whereas other antiviral drugs such as oseltamivir, and ganciclovir have been

tested for treatment of some patients in Wuhan hospital [11]. Remdesivir has been recently recognized as a promising antiviral drug against a wide array of RNA viruses (including SARS/MERS-CoV) [12-14].

Additionally, Xiao *et al.* [15] have reported that remdesivir and chloroquine effectively inhibit the novel coronavirus (2019-nCoV) in vitro. Slutsky *et al.* [16] have reviewed the rationale for angiotensin-converting enzyme 2 (ACE2) receptor as a SARS-CoV-2 receptor, since it has many similarities with the original SARS-CoV and the latter spike protein has a strong binding affinity to human ACE2, based on biochemical interaction studies and crystal structure analysis.

Since it has been reported that some drugs can be used as anti-SARS drugs by targeting 3CLpro (3-chymotrypsin-like cysteine protease) and RNA-dependent RNA polymerase (RdRp) of SARS-CoV-2, we have selected five drugs as well as the proposed remdesivir analogue (AZCV-20) to investigate their binding interactions with 3CLpro and (RdRp), and to evaluate their potential against coronavirus pneumonia (SARS-CoV-2) infection by means of computational methods using two docking tools, MOE 2105 and Autodock [17].

## 2. Materials and Methods

The crystal structures of SARS-CoV-2 (PDB code: 6LU7) 3CLpro and SARS-CoV Nsp12 polymerase (PDB code: 6NUR) were obtained from the Protein Data Bank ([www.pdb.org](http://www.pdb.org)). The molecular docking programs MOE 2105 and Autodock [17] were used in this work. For docking analysis, the studied ligands were sketched using MOE 2105 interface and their molecular structures were optimized with the MMFF94x force field [18]. For calculating the atomic charges of the studied ligands their geometries were fully optimized with the B3LYP [19, 20] functional in conjunction with the 6-311+G(d,p) basis set using the Gaussian 16 [21] package of programs. The optimized structures were used as inputs for the AIMAll [22] program in order to calculate atomic charges  $q(A)$ . Before docking water molecules and metals were stripped out from the proteins pdb files while missing side chains and residues were fixed and protein energies were minimized using the Amber10 forcefield. The resulted structures were used for docking analysis in both MOE 2015 and Autodock programs.

## 3. Results and Discussion

Severe acute respiratory syndrome coronavirus (SARS-CoV-2) viral 3-chymotrypsin-like cysteine protease (3CLpro) enzyme, a protein required for the maturation of SARS-CoV, is vital for its life cycle, making it an attractive target for structure-based drug design of anti-SARS drugs. In Feb. 2020, Li *et al.* [23] have studied the interactions of some antiviral drugs and natural products with SARS-CoV-2 by computational methods. Monajjemi *et al.* [24] have reported the binding of some inhibitors as antiviruses isolated from Gillan's plants with coronavirus NSP12 bound to NSP7 and NSP8 co-factors, while the same group have studied the modelling and simulation of all COVID-19 proteins, receptors, S proteins including s1 and s2 via molecular docking study [25]. In our study, we have selected five drugs with their isomers: remdesivir, (*R*)-chloroquine, (*S*)-chloroquine, (*R*)-hydroxychloroquine, (*S*)-hydroxychloroquine, umifenovir and favipiravir, in addition to the proposed remdesivir analogue namely, AZCV-20 (Figure 1) for their virtual molecular docking with the SARS-COVID-19 protease and polymerase enzymes. Table 1 shows the binding energy score for these drugs with

SARS-CoV-2 3CLpro (PDB code: 6LU7) and RdRp (PDB code: 6NUR) calculated by MOE and Auodock4 methods.

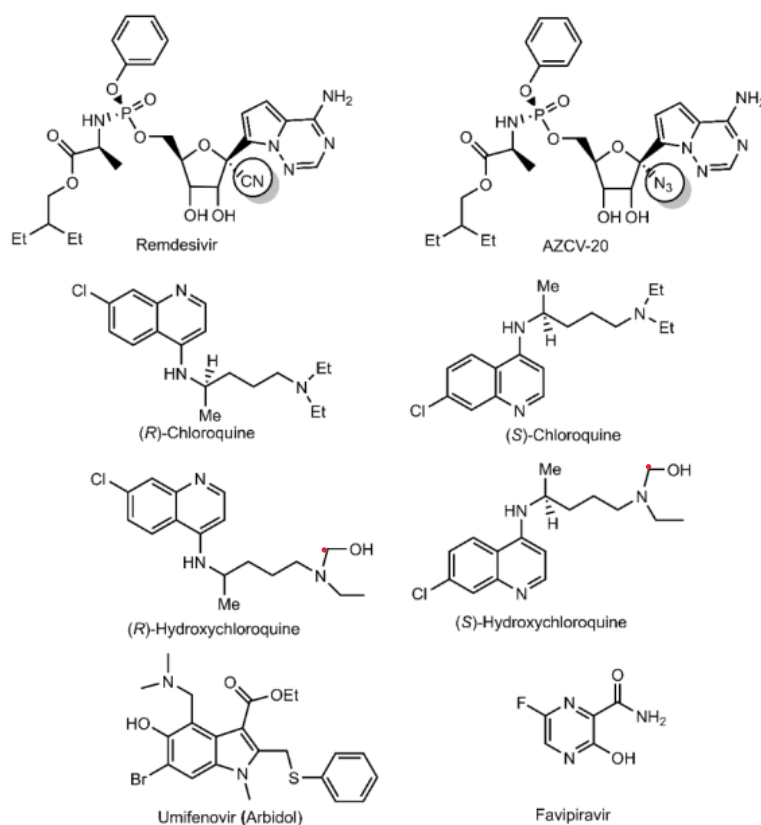


**Figure 1.** Chemical structures of some drugs used in this study. Remdesivir, Remdesivir analog (AZCV-20), (*R* and *S*)-Chloroquine, (*R* and *S*)-Chloroquine, (*R* and *S*)-Hydroxychloroquine, Umifenovir (Arbidol), Favipiravir.

### 3.1. Docking of remdesivir.

*In vitro* study published in January has shown remdesivir to be active against a clinical isolate of SARS-CoV-2 [12-14]. Remdesivir has been shown to reduce the severity of disease, virus replication and damage to the lungs in a non-human primate model of MERS. For both tools MOE 2015 and Autodock docking study with the SARS-CoV-2 3CLpro structure (PDB code: 6LU7) [26, 27] and RdRp structure (PDB code: 7NUR), remdesivir bound strongly to the receptor binding site of both SARS-CoV 3CLpro and RdRp (Figures 2A, and 2B). The generated docking showed relatively high scores of remdesivir (-8.3219 and -8.4299 kcal. mol<sup>-1</sup>, PDB codes: 6LU7 and 7NUR, MEO 2015, respectively), and (-9.41 and -9.23 kcal. mol<sup>-1</sup>, PDB codes: 6LU7 and 7NUR, Autodock, respectively). The docking models of 3CLpro (PDB code: 6LU7) illustrated that the carbonyl group of alkyl phosphonate of remdesivir made a strong H-bond with Gly143 (2.15 Å). In addition, the OH at C-3 of ribose moiety and NH<sub>2</sub> of pyrrolo-triazine of remdesivir were hydrogen bonded with Leu271 (2.33 Å), and Met666 (2.73 Å) of RdRp (PDB code: 7NUR) along with the other residues.

### 3.2. Docking of AZCV-20.

For the theoretical study, we have designed a new remdesivir analogue, namely (AZCV-20), by substitution of the nitrile group at C-1 of the ribose moiety of remdesivir by the azide residue (Figure 1). As described for remdesivir, the same strategy was employed to identify the score structure. AZCV-20 demonstrated best docking pose based on docking score using MEO method (-9.7613, and -8.6878 kcal.mol<sup>-1</sup>) of PDB codes: 6LU7 and 7NUR, respectively, in

comparison for those scores determined by Autodock (Table 1). In addition, AZCO-20 exhibited the highest binding affinity ( $-10.44 \text{ kcal.mol}^{-1}$ ) in comparison for those of remdesivir, with a competitive inhibition value of  $K_i$   $22.38 \text{ nM}$ . The predicted model showed a strong H-bond between the oxygen of ( $\text{PO}_3\text{NH}$ ) group and Glu166 ( $2.04 \text{ \AA}$ ) together with a hydrophobic interaction between H-arene of the triazine ring and His41 (Figures 2C and 2D).

### 3.3. Docking of (*R* and *S*)-Chloroquine and (*R* and *S*)-hydroxychloroquine.

These drugs have been found to be efficient in Chinese SARS-CoV-2 patients [28, 29]. Therefore, we decided to generate docking models of both (*R*) and (*S*) isomers of chloroquine and hydroxychloroquine separately. As shown in Table 1, (*R*)- and (*S*)-chloroquines have been proved to have a better binding affinity with SARS-CoV-2 RdRp (PDB code: NUR) ( $-7.14$ , and  $-7.40 \text{ kcal.mol}^{-1}$ ), respectively, using Autodock method, meanwhile their binding energy values are close to each other, and the competitive inhibition ( $K_i$ ) of both isomers =  $5.57$  and  $3.77 \text{ \mu M}$ , respectively. As suggested by the model and visualized in Figures 2F and 2H, docking study of (*R*)- and (*S*)-chloroquines have shown satisfactory results. There are two H-bonds ( $3.35$  and  $3.72 \text{ \AA}$ ) between Thr394 of RdRp and Cl residue of both isomers of the drug, in addition to two backbone donor interactions between Phe396, Pro677 and CH of pyridine. Although (*R*)-hydroxychloroquine showed a higher binding score ( $-7.2664 \text{ kcal.mol}^{-1}$ ) with 3CLpro than those of the (*S*)-isomer ( $-7.0748 \text{ kcal.mol}^{-1}$ ), using MEO method, but the latter has a competitive inhibition ( $K_i$ ) value of  $61.07 \text{ \mu M}$  ( $K_i$  of *R*-isomer  $150.86 \text{ \mu M}$ ). However, the binding modes of isomers (*R* and *S*)-hydroxychloroquine in their docking complexes are shown in (Figures 2I-2L). As revealed in the docking model of (*R*)-hydroxychloroquine, a strong H-bond between OH group and Thr26 ( $2.39 \text{ \AA}$ ) of 3CLpro (PDB code: 6LUR) was observed, and made close contact with His41, as well as interactions with receptor-binding residues Gln189, Met49, Ser46, Cys145, Ser144, Thr25, Met165, Thr26, His163, His41, Leu27, Gly143, His172, Leu141, Glu166, His164, Phe140, Asn142 and Gln189 (Fig. 2I). These results confirmed our findings, and further indicate that chloroquine and hydroxychloroquine may serve as potential anti-SARS-CoV-2 drug sources.

### 3.4. Docking of umifenovir.

It is an antiviral drug and being studied in Feb. 2020 in patients trial in China for treatment of the SARS-CoV-2. Chinese experts claimed that preliminary tests had shown that umifenovir (arbidol) and darunavir could inhibit replication of the virus [30], since there is evidence to prevent infections from RNA viruses than infections from DNA viruses [31]. As shown in (Figures 2M and 2N), umifenovir was docked in the binding cavity of the both SARS-CoV-2 3CLpro and RdRp enzymes with two H-bonds. Uminfenovir exhibited a strong H-bond between the OH group of indole ring and Glu166 ( $2.15 \text{ \AA}$ ) of 3CLpro (PDB code: 6LU7), meanwhile the drug is located in the middle of the binding pocket inserted deep into the hydrophobic pocket consisting of residues Gln189, Ser144, Phe140, Leu141, Asn142, His163, Glu166, Met165, His164, Asp187, Arg188, Tyr54, Met49, His41, Gly143, and Cys145. In addition, a strong interaction between methyl group and Asp760 ( $2.22 \text{ \AA}$ ) of RdRp (PDB code: 7NUR) as well as interactions with receptor-binding residues Thr556, Asp623, Arg555, Cys622, Ala554, Asp761, Asp760, Ser759, Asn691, Tyr619, and Leu758. These results suggest that umifenovir be a promising useful candidate for SARS-CoV-2 drug therapy.

### 3.5. Docking of favipiravir.

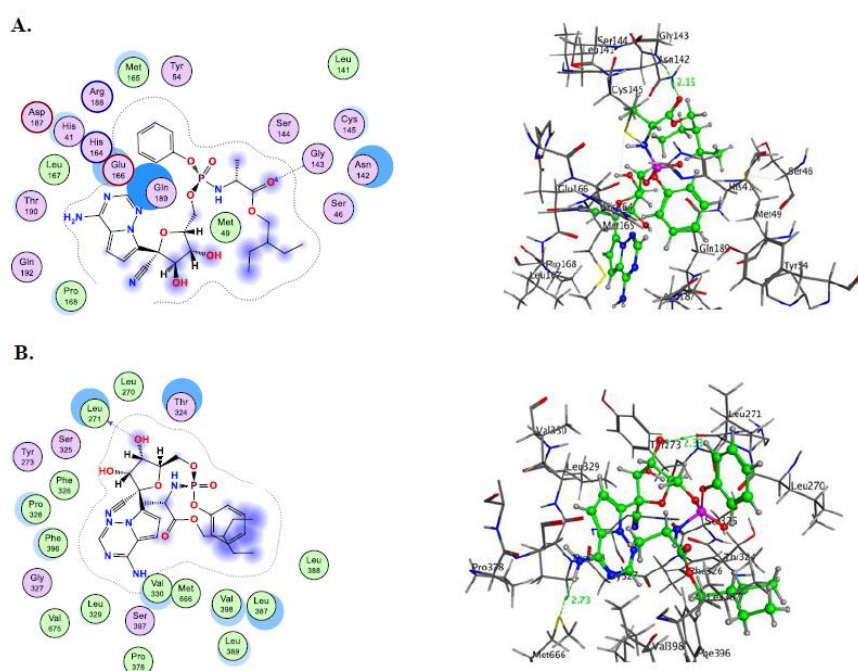
It is an antiviral drug being developed by Toyama Chemical of Japan with activity against many RNA viruses [32, 33]. In February 2020, favipiravir was being studied in China for experimental treatment of the emergent SARS-CoV-2 disease [5, 34]. In March 2020, Chinese officials concluded favipiravir is clearly effective in treating the novel coronavirus.

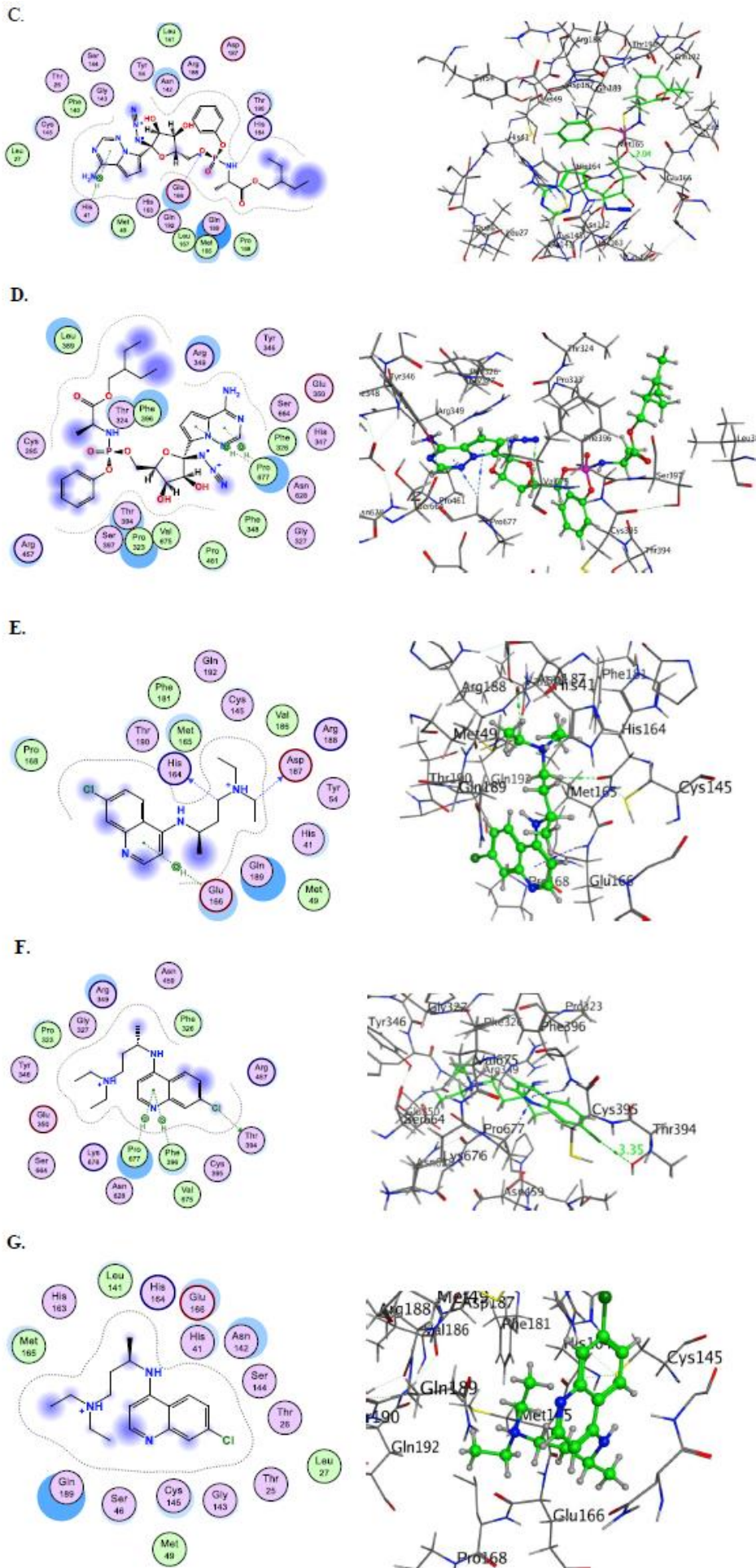
From the generated docking model, it was predicted that favipiravir bounded in the active site of the SARS-CoV-2 3CLpro (PDB code: 6LU7). Figures 2O and 3P demonstrated a strong H-bond between NH<sub>2</sub> group of the amide residue and Ser343 (2.28 Å). Overall, the combination of hydrophobic interactions of Met49, Gln189, Asp187, His41, Val186, Met165, Arg188, Tyr54, Phe181, His164 and pi-stacking appears to govern the binding of favipiravir with 3CLpro enzyme. Additionally, the docking of SARS-CoV-2 RdRp (PDB code: 7NUR) with favipiravir revealed a H-bond between oxygen atom of the amide group and Gln200 (2.21 Å), as well as extensive hydrophobic interactions with the surrounding residues including Ser343, Tyr530, Asp358, Ile536, Val359, Val373, Glu370, Leu527, Tyr374, Lys369, Thr344, and Asn356.

**Table 1.** The docking scores of some drugs with 3-CLpro and RdRp of COVID-19 calculated by MOE and Autodock programs.

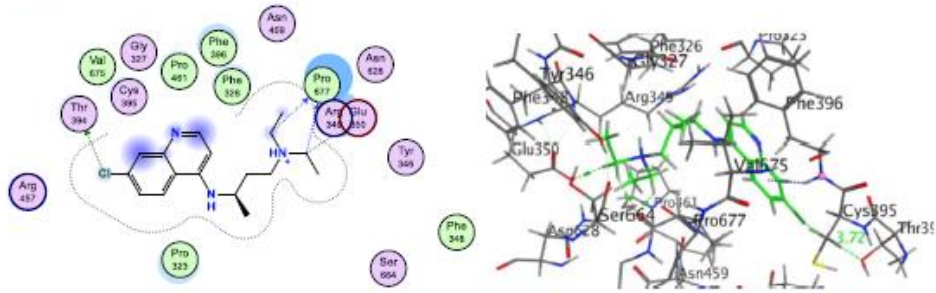
Drug	MOE 2015	MOE 2015	Autodock	Autodock
	6LU7	7NUR	6LU7	7NUR
Remdesivir	-8.3219	-8.4299	-9.70	-9.03
AZCV-20	-9.7613	-8.6878	-10.44	-9.43
S-Chloroquine	-6.5157	-6.9088	-5.95	-7.40
R-Chloroquine	-5.9884	-7.1286	-5.75	-7.14
S-Hydroxychloroquine	-7.0748	-6.8146	-5.21	-6.08
R-Hydroxychloroquine	-7.2664	-7.1132	-5.21	-6.08
Umifenovir	-6.8199	-7.1245	-6.64	-8.51
Favipiravir	-4.8818	-5.7472	-4.78	-5.59

Tables 2 and 3 illustrate the binding energies, docking energies, and inhibition constant values of the drugs calculated by MOE and Autodock4 tools, respectively, whereas Table 4 presented the physical interactions of some drugs with the active site of amino acids of SARS-CoV-2.

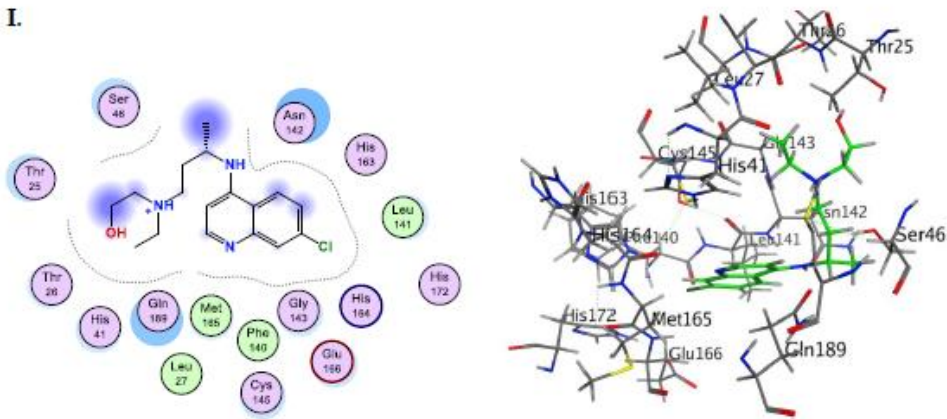




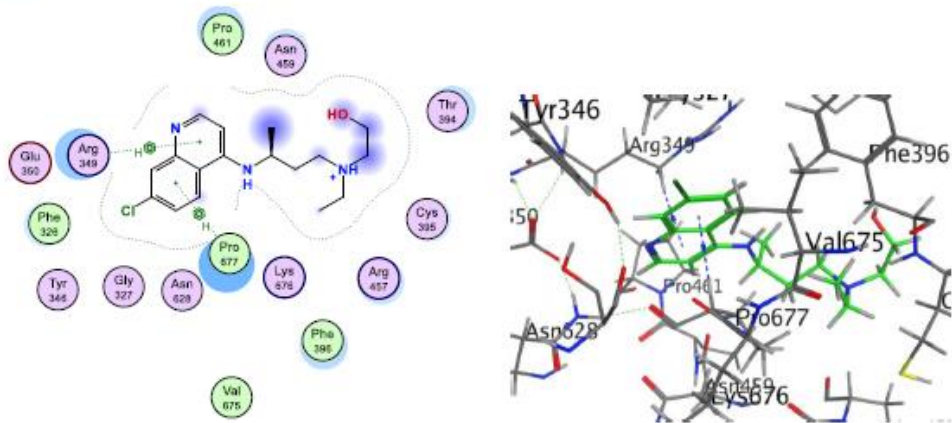
**H.**



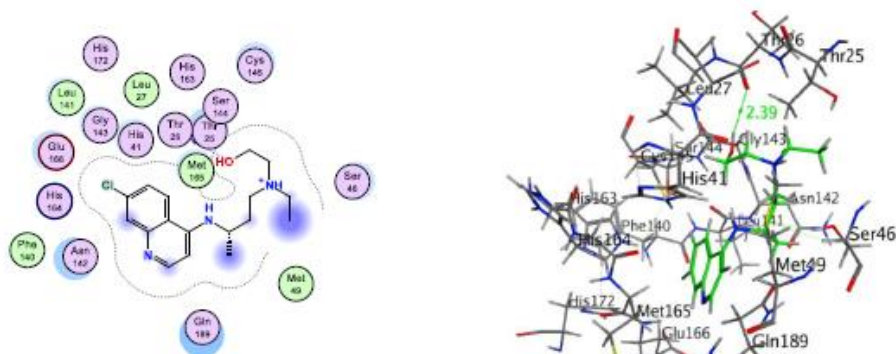
**I.**



**J.**



**K.**



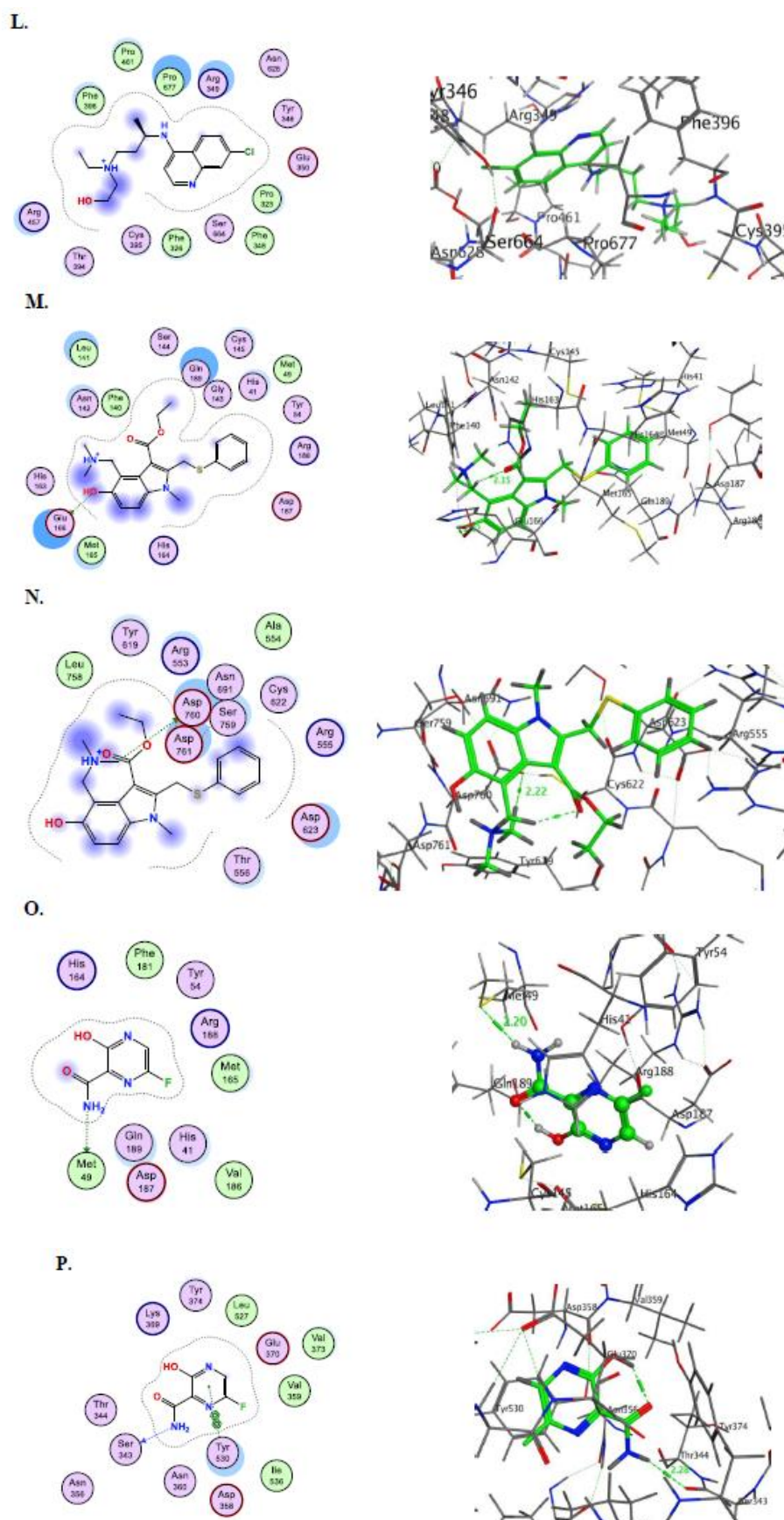


**Figure 2.** Structure of SARS-COVID-19 3CLpro (PDB code: 6LU7) and RdRp (PDB code: 7NUR) enzymes in complexes with drugs: **A.** Remdesivir + 6LU7; **B.** Remdesivir + 7NUR, **C.** AZCV-20 + 6LU7, **D.** AZCV-20 + 7NUR, **E.** (*R*)-Chloroquine + 6LU7; **F.** (*R*)-Chloroquine + 7NUR, **G.** (*S*)-Chloroquine + 6LU7, **H.** (*S*)-Chloroquine + 7NUR; **I.** (*R*)-Hydroxychloroquine + 6LU7, **J.** (*R*)-Hydroxychloroquine + 7NUR, **K.** (*S*)-Hydroxychloroquine + 6LU7; **L.** (*S*)-Hydroxychloroquine + 7NUR; **M.** Umifenovir (Arbidol) + 6LU7; **N.** Umifenovir (Arbidol) + 7NUR; **O.** Favipiravir + 6LU7; **O.** Favipiravir + 7NUR.



**Table 2.** Binding energies,  $K_i$ , and inhibition constant values of some drugs at  $T = 298.5$  K calculated by Auodock4 (PDB ID: 6LU7).

Drug	$K_i$ (xM)	Binding energy*	Intramolecular Energy*	Internal Energy*	Torsional Energy*	Unbound external energy*
Remdesivir	78.21 nM	-9.70	-10.83	-5.87	5.07	-1.94
AZCV-20	22.38 nM	-10.44	-10.02	-7.56	5.37	-1.78
(S)-Chloroquine	24.61 $\mu$ M	-6.29	-7.41	-1.22	2.07	-0.25
(R)-Chloroquine	43.86 $\mu$ M	-5.95	-7.56	-0.61	2.09	-0.14
(S)-Hydroxy-chloroquine	61.07 $\mu$ M	-5.75	-8.16	-0.74	2.68	-0.46
(R)-Hydroxy-chloroquine	150.86 $\mu$ M	-5.21	-7.75	-0.58	2.68	-0.43
Umifenovir	13.68 $\mu$ M	-6.64	-8.02	-2.06	2.68	-0.76
Favipiravir	315.59 $\mu$ M	-4.78	-4.87	-0.53	0.60	-0.04

<sup>a</sup> The energy values are in kcal.mol<sup>-1</sup>.

**Table 3.** Binding energies,  $K_i$ , and inhibition constant values of some drugs at  $T = 298.5$  K calculated by Auodock4 (PDB ID: 6NUR).

Drug	$K_i$ (xM)	Binding energy*	Intramolecular Energy*	Internal Energy*	Torsional Energy*	Unbound external energy*
Remdesivir	240.74 nM	-9.03	-9.97	-6.01	5.07	-1.88
AZCV-20	121.56 nM	-9.43	-9.81	-6.77	5.37	-1.77
(R)-Chloroquine	5.57 $\mu$ M	-7.17	-8.89	-0.62	2.09	-0.13
(S)-Chloroquine	3.77 $\mu$ M	-7.40	-8.94	-0.68	2.09	-0.13
(R)-Hydroxy-chloroquine	3.77 $\mu$ M	-7.14	-9.70	-0.58	2.68	-0.46
(S)-Hydroxy-chloroquine	35.0 $\mu$ M	-6.08	-8.52	-0.67	2.68	-0.42
Umifenovir	577.25 nM	-8.51	-10.-8	-1.96	2.68	-0.85
Favipiravir	79.44 $\mu$ M	-5.59	-5.22	-1.02	0.60	-0.04

<sup>a</sup> The energy values are in kcal mol<sup>-1</sup>.

**Table 4.** Physical interactions of some drugs with the active site of amino acids of SARS-CoV-2.

Drug	Residues interacting with Ligand through H-Bonding and other interactions (PDB ID)	Physical interactions; bond lengths (R) Alkyl-Pi interactions
Remdesivir	<b>6LU7:</b> Gly143, Ser46, Asn142, Cys145, Leu141, ser144, Tyr54, Met165, Arg188, Met49, Gln189, Glu166, His614, His41, Asp187, Leu167, thr190, Gln192, Pro168, <b>6NUR:</b> Val330, Met666, Val398, Leu387, Ser397, Pro378, Leu380, Leu388, Thr324, Leu270, Leu271, Ser325, Tyr273, Phe326, Pro328, Phe396, Gly327, val675, Leu329.	RCO-Gly143 = 2.15 Å ROH-Leu271 = 2.33 Å RNH2-Met666 = 2.73 Å
AZCV-20	<b>6LU7:</b> His41, Met49, His163, Gln192, Glu166, Leu167, Met165, Gln189, Pro168, His164, Thr190, Asp187, Arg188, Leu141, Tyr54, Asn142, Gly143, Ser144, Gly143, Phe140, Thr26, Cys145, Leu27. <b>6NUR:</b> Thr394, Ser397, Pro323, val675, Pro461, Phe348, Gly327, Asn628, Pro677, Phe326, His347, Ser664, Glu350, Tyr346, Arg349, Phe396, Thr324, Leu398, Cys395, Arg457	RO-Glu166 = 2.04 Å His41 arene-H with the triazine rings 2XPro677 (CH-pi) or arene-H with the triazine rings
(S)-Chloro- quine	<b>6LU7:</b> Glu166, Gln189, Met49, His41, Tyr54, Asp187, Arg188, Val186, Cys145, Gln192, Phe181, Thr190, Pro168. <b>6NUR:</b> Pro677, Phe396, Val675, Cys395, Thr394, Arg457, Phe326, Asn459, Arg349, Gly327, Pro323, Tyr346, Glu350, Ser664, Lys676, Asn628.	Glu166 arene-H His164-CH (backbone donor) Asp187-CH (backbone donor) Phe396 arene-H Pro677 arene-H RCI-Thr394 = 3.35 Å
(R)-Chloro- quine	<b>6LU7:</b> Gln189, Ser46, Cys145, Met49, Gly143, Thr25, Leu27, Thr26, Ser144, Asn142, His41, Glu166, His164, Leu141, His163, Met165. <b>7NUR:</b> Pro323, Ser664, Tyr346, Glu350, Arg349, Pro677, Asn628, Asn459, Phe326, Phe396, Pro461, Gly327, Cys395, Val675, Thr394, Arg457.	--- RCI-Thr394 = 3.72 Å Pro677-CH (backbone donor) Phe396 arene-H
(S)-Hydroxy- chloroquine	<b>6LU7:</b> Gln189, Met49, Ser46, Cys145, Ser144, Thr25, Met165, Thr26, His163, His41, Leu27, Gly143, His172, Leu141, Glu166, His164, Phe140, Asn142. <b>6NUR:</b> Val675, Phe396, Pro677, Lys676, Arg457, Cys395, Thr394, Asn459, Pro461, Arg349, Glu350, Glu350, Phe326, Tyr346, Gly327, Asn628.	ROH-Thr26 = 2.39 Å Arg349 arene-H Pro677 arene-H

( <i>R</i> )-Hydroxy-chloroquine	<b>6LU7:</b> Gln189, Met49, Ser46, Cys145, Ser144, Thr25, Met165, Thr26, His163, His41, Leu27, Gly143, His172, Leu141, Glu166, His164, Phe140, Asn142. <b>6NUR:</b> Val675, Phe396, Pro677, Lys676, Arg457, Cys395, Thr394, Asn459, Pro461, Arg349, Glu350, Glu350, Phe326, Tyr346, Gly327, Asn628.	---
Umifenovir	<b>6LU7:</b> Gln189, Ser144, Phe140, Leu141, Asn142, His163, Glu166, Met165, His164, Asp187, Arg188, Tyr54, Met49, His41, Gly143, Cys145. <b>6NUR:</b> Thr556, Asp623, Arg555, Cys622, Ala554, Asp761, Asp760, Ser759, Asn691, Tyr619, Leu758.	R <sub>OH-Glu166</sub> = 2.15 Å R <sub>CH3-Asp760</sub> = 2.22 Å
Favipiravir	<b>6LU7:</b> Met49, Gln189, Asp187, His41, Val186, Met165, Arg188, Tyr54, Phe181, His164. <b>6NUR:</b> Ser343, Tyr530, Asp358, Ile536, Val359, Val373, Glu370, Leu527, Tyr374, Lys369, Thr344, Asn356	R <sub>NH2-Ser343</sub> = 2.28 Å Tyr530 aren-aren R <sub>C=O-Gln200</sub> = 2.21 Å

DFT calculations were performed for both isomers of chloroquine and hydroxychloroquine. Optimized molecular structures of the most stable forms are shown in Figure 3.

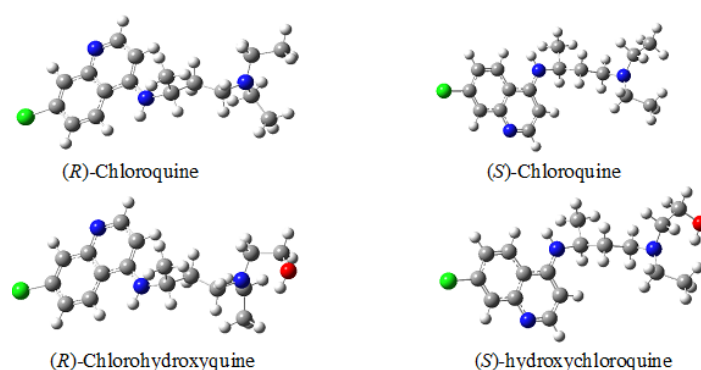


**Figure 3.** The optimized molecular structures of (*R*)-chloroquine, (*S*)-chloroquine, (*R*)-hydroxy-chloroquine, and (*S*)-hydroxychloroquine.

Figure 4 and Table 5 summarized the atomic charges (qA) of these drugs calculated by AIMAll program (according to Bader Atoms-in-Molecules theory) (**Supplementary data**).

#### 4. Conclusions

In this study, we have selected five pharmaceuticals with their isomers, remdesivir, chloroquine, hydroxychloroquine, umifenovir and favipiravir, in addition to our proposed analogue (AZCV) as inhibitor drugs for the novel coronavirus SARS-CoV-2 to evaluate and compare their energy scores and binding affinity with SARS-CoV 3CLpro and RdRp enzymes by molecular docking, using MEO and Autodock4 methods. Our results showed that all of these drugs formed H-binding interactions with the SARS-CoV-2 3CLpro and RdRp enzymes, predicting the possibility to become SARS-CoV-2 inhibitors. However, we need further study to verify this conclusion.

#### Funding

This research received no external funding.

#### Acknowledgments

This project is supported by Basrah University, Iraq, during their projects strategy to inhibit the novel SARS-CoV-2.

## Conflicts of Interest

The authors declare no conflict of interest.

## References

1. Huang, C.; Wang, Y.; Li, X.; Ren, L.; Zhao, J.; Hu, Y.; Zhang, L.; Fan, G.; Xu, J.; Gu, X.; Cheng, Z.; Yu, T.; Xia, J.; Wei, Y.; Wu, W.; Xie, X.; Yin, W.; Li, H.; Liu, M.; Xiao, Y.; Gao, H.; Guo, L.; Xie, J.; Wang, G.; Jiang, R.; Gao, Z.; Jin, Q.; Wang, J.; Cao, B. Clinical features of patients infected with 2019 novel coronavirus in Wuhan, China. *Lancet* **2020**, *395*, 497-506, [https://doi.org/10.1016/S0140-6736\(20\)30183-5](https://doi.org/10.1016/S0140-6736(20)30183-5).
2. Zhu, N.; Zhang, D.; Wang, W.; Li, X.; Yang, B.; Song, J.; Zhao, X.; Haung, B. China novel coronavirus investigating and research team. A novel coronavirus from patients with pneumonia in China, 2019. *N. Engl. J. Med.* **2020**, *382*, 727-733, <https://doi.org/10.1056/NEJMoa2001017>.
3. Gao, J.; Tian, Z.; Yang, X. Breakthrough: chloroquine phosphate has shown apparent efficacy in treatment of COVID-19 associated pneumonia in clinical studies. *Biosci. Trends* **2020**, *14*, 72-73, <https://doi.org/10.5582/bst.2020.01047>.
4. Colson, P.; Rolain, J.M.; Lagier, J.C.; Brouqui, P.; Raoult, D. Chloroquine and hydroxychloroquine as available weapons to fight COVID-19. *Int. J. Antimicrob. Agents* **2020** Mar 4, in press 105932. <https://doi.org/10.1016/j.ijantimicag.2020.105932>.
5. Li, G.; De Clercq, E. Therapeutic options for the 2019 novel coronavirus (2019-nCoV). *Nat. Rev. Drug Discov.* **2020**, *19*, 149-150, <https://doi.org/10.1038/d41573-020-00016-0>.
6. Xu, X.; Chen, P.; Wang, J.; Feng, J.; Zhou, H.; Li, X.; Zhong, W.; Hao, P. Evolution of the novel coronavirus from the ongoing Wuhan outbreak and modeling of its spike protein for risk of human transmission. *Sci. China Life Sci.* **2020**, in press. <https://doi.org/10.1007/s11427-020-1637-5>.
7. Reddy, A.D.; Suh, S.B.; Ghaffari, R.; Singh, N.J.; Kim, D.J.; Han, J.H. Bioinformatics analysis of SARS proteins and molecular dynamics simulated structure of an alpha-helix motif. *Bull. Korean Chem. Soc.* **2003**, *24*, 899-900, <https://doi.org/10.5012/bkcs.2003.24.7.899>.
8. Xia, B.; Kang, X. Activation and maturation of SARS-CoV main protease. *Protein & cell.* **2011**, *2*, 282-90, <https://doi.org/10.1007/s13238-011-1034-1>.
9. Lu, I.L.; Mahindroo, N.; Liang, P.H.; Peng, Y.H.; Kuo, C.J.; Tsai, K.C.; Hsieh, H.P.; Chao, Y.S.; Wu, S.Y. Structure-based drug design and structural biology study of novel nonpeptide inhibitors of severe acute respiratory syndrome coronavirus main protease. *J. Med. Chem.* **2006**, *49*, 5154-61, <https://doi.org/10.1021/jm060207o>.
10. Zumla, A.; Chan, J.F.; Azhar, E.I.; Hui, D.S.; Yuen, K.Y. Coronaviruses - drug discovery and therapeutic options. *Nat. Rev. Drug Discov.* **2016**, *15*, 327-347, <https://doi.org/10.1038/nrd.2015.37>.
11. Wu, C.; Chen, X.; Cai, Y.; Xia, J.a.; Zhou, X.; Xu, S.; Huang, H.; Zhang, L.; Zhou, X.; Du, C.; Zhang, Y.; Song, J.; Wang, S.; Chao, Y.; Yang, Z.; Xu, J.; Zhou, X.; Chen, D.; Xiong, W.; Xu, L.; Zhou, F.; Jiang, J.; Bai, C.; Zheng, J.; Song, Y. Risk factors associated with acute respiratory distress syndrome and death in patients with coronavirus disease 2019 pneumonia in Wuhan, China. *JAMA Intern. Med.* **2020**, in press. <https://doi.org/10.1001/jamainternmed.2020.0994>.
12. Sheahan, T.P.; Sims, A.C.; Graham, R.L.; Menachery, V.D.; Gralinski, L.E.; Case, J.B.; Leist, S.R.; Pyrc, K.; Feng, J.Y.; Trantcheva, I.; Bannister, R.; Park, Y.; Babusis, D.; Clarke, M.O.; Mackman, R.L.; Spahn, J.E.; Palmiotti, C.A.; Siegel, D.; Ray, A.S.; Cihlar, T.; Jordan, R.; Denison, M.R.; Baric, R.S. Broad-spectrum antiviral GS-5734 inhibits both epidemic and zoonotic coronaviruses. *Sci. Transl. Med.* **2017**, *9*, eaal3653. <https://doi.org/10.1126/scitranslmed.aal3653>.
13. Agostini, M.L.; Andres, E.L.; Sims, A.C.; Graham, R.L.; Sheahan, T.P.; Lu, X.; Smith, E.C.; Case, J.B.; Feng, J.Y.; Jordan, R.; Ray, A.S.; Cihlar, T.; Siegel, D.; Mackman, R.L.; Clarke, M.O.; Baric, R.S.; Denison, M.R. Coronavirus Susceptibility to the Antiviral Remdesivir (GS-5734) is mediated by the viral polymerase and the proofreading exoribonuclease. *mBio* **2018**, *9*, e00221, <https://doi.org/10.1128/mBio.00221-18>.
14. Brown, A.J.; Won, J.J.; Graham, R.L.; Dinnon, K.H.; Sims, A.C.; Feng, J.Y.; Cihlar, T.; Denison, M.R.; Baric, R.S.; Sheahan, T.P. Broad spectrum antiviral remdesivir inhibits human endemic and zoonotic deltacoronaviruses with a highly divergent RNA dependent RNA polymerase. *Antiviral Res.* **2019**, *169*, <https://doi.org/10.1016/j.antiviral.2019.104541>.
15. Wang M, Cao R, Zhang L, Yang X, Liu J, Xu M, Shi Zh, Hu Zh, Zhong W, Xiao G. Remdesivir and chloroquine effectively inhibit the recently emerged novel coronavirus (2019-nCoV) *in vitro*. *Cell Res.* **2020**, *30*, 269-271, <https://doi.org/10.1038/s41422-020-0282-0>.
16. Zhang, H.; Penninger, J.M.; Li, Y.; Zhong, N.; Slutsky, A.S. Angiotensin-converting enzyme 2 (ACE2) as a SARS-CoV-2 receptor: molecular mechanisms and potential therapeutic target. *Intensive Care Med.* **2020**, *46*, 586-590, <https://doi.org/10.1007/s00134-020-05985-9>.
17. Morris, G.M.; Huey, R.; Lindstrom, W.; Sanner, M.F.; Belew, R.K.; Goodsell, D.S.; Olson, A.J.J. AutoDock4 and AutoDockTools4: Automated docking with selective receptor flexibility. *Comput. Chem.* **2009**, *30*, 2785-2791, <https://doi.org/10.1002/jcc.21256>.

18. Halgren, T.A. Merck molecular force field: I. basis, form, scope, parameterization and performance of MMFF94. *J. Comp. Chem.* **1996**, *17*, 490-519, [https://doi.org/10.1002/\(SICI\)1096-987X\(199604\)17:5/6<490::AID-JCC1>3.0.CO;2-P](https://doi.org/10.1002/(SICI)1096-987X(199604)17:5/6<490::AID-JCC1>3.0.CO;2-P).
19. Becke, A.D. Density-functional thermochemistry. III. The role of exact exchange. *J. Chem. Phys.* **1993**, *98*, 5648-5652, <https://doi.org/10.1063/1.464913>.
20. Lee, C.; Yang, W.; Parr, R.G. Development of the Colle-Salvetti correlation-energy formula into a functional of the electron density. *Phys. Rev. B* **1988**, *37*, 785-789. <https://doi.org/10.1103/PhysRevB.37.785>.
21. Frisch, M.J.; Trucks, G.W.; Schlegel, H.B.; Scuseria, G.E.; Robb, M.A.; Cheeseman, J.R.; Scalmani, G.; Barone, V.; Petersson, G.A.; Nakatsuji, H. Gaussian 16 Rev. B.01, Wallingford, CT, 2016.
22. AIMAll (Version 19.10.12), Todd, A.; Keith, T.K. Gristmill Software, Overland Park KS, USA, 2019 ([aim.tkgristmill.com](http://aim.tkgristmill.com)).
23. Wu, C.; Liu, Y.; Yang, Y.; Zhang, P.; Zhong, W.; Wang, Y.; Wang, Q.; Xu, Y.; Li, M.; Li, X.; Zheng, M.; Chen, L.; Li, H. Analysis of therapeutic targets for SARS-CoV-2 and discovery of potential drugs by computational methods. *Acta Pharm, Sinica, B* **2020**, in press. <https://doi.org/10.1016/j.apsb.2020.02.008>.
24. Monajjemi, M.; Mollaamin, F.; Shojaei, S. An overview on Coronaviruses family from past to Covid-19: introduce some inhibitors as antiviruses from Gillan's plants. *Biointerface Res.Appl. Chem.* **2020**, *10*, 5575-5585, <https://doi.org/10.33263/BRIAC103.575585>.
25. Monajjemi, M.; Shahriari, S.; Mollaamin, F. Evaluation of Coronavirus families & Covid-19 proteins: molecular modeling study. *Biointerface Res.Appl. Chem.* **2020**, *10*, 6039- 6057, <https://doi.org/10.33263/BRIAC105.60396057>.
26. Berman, H.M.; Westbrook, J.; Feng, Z.; Gilliland, G.; Bhat, T.N.; Weissig, H.; Shindyalov, I.N.; Bourne, P.E. The Protein Data Bank. *Nucleic Acids Res.* **2000**, *28*, 235-242, <https://doi.org/10.1093/nar/28.1.235>.
27. Liu, X.; Zhang, B.; Jin, Z.; Yang, H.; Rao, Z. The crystal structure of 2019-nCoV main protease in complex with an inhibitor N3. *Protein Data Bank (PDB)* **2020**, <https://doi.org/10.2210/pdb6lu7/pdb>.
28. Wang, M.; Cao, R.; Zhang, L. Yang, X.; Liu, J.; Xu, M.; Shi, Z.; Hu, Z., Zhong, W., Xiao, G. Remdesivir and chloroquine effectively inhibit the recently emerged novel coronavirus (2019-nCoV) in vitro. *Cell Res.* **2020**, *30*, 269-271, <https://doi.org/10.1038/s41422-020-0282-0>.
29. Gautret, P.; Lagier, J.C.; Parola, P.; Hoang, V.T.; Meddeb, L.; Mailhe, M.; Doudier, B.; Courjon, J.; Giordanengo, V.; Vieira, V.E.; Dupont, H.T.; Honoré, S.; Colson, P.; Chabrière, E.; La Scola, B.; Rolain, J.-M.; Brouqui, P.; Raoult, D. Hydroxychloroquine and azithromycin as a treatment of COVID-19: results of an open-label non-randomized clinical trial. *Int. J Antimicrob. Agents* **2020**; in press. <https://doi.org/10.1016/j.ijantimicag.2020.105949>.
30. Lu, H. Drug treatment options for the 2019-new coronavirus (2019-nCoV). *Biosci. Trends* **2020**, *14*, 69-71, <https://doi.org/10.5582/bst.2020.01020>.
31. Shi, L.; Xiong, H.; He, J.; Deng, H.; Li, Q.; Zhong, Q.; Hou, W.; Cheng, L.; Xiao, H.; Yang, Z. Antiviral activity of arbidol against influenza A virus, respiratory syncytial virus, rhinovirus, coxsackie virus and adenovirus in vitro and in vivo. *Arch. Virolo.* **2007**, *152*, 1447-55, <https://doi.org/10.1007/s00705-007-0974-5>.
32. Furuta, Y.; Takahashi, K.; Shiraki, K.; Sakamoto, K.; Smee, D.F.; Barnard, D.L.; Gowen, B.B.; Julander, J.G.; Morrey, J.D. T-705 (favipiravir) and related compounds: Novel broad-spectrum inhibitors of RNA viral infections. *Antiviral Res.* **2009**, *82*, 95-102, <https://doi.org/10.1016/j.antiviral.2009.02.198>.
33. Furuta, Y.; Gowen, B.B.; Takahashi, K.; Shiraki, K.; Smee, D.F.; Barnard, D.L. Favipiravir (T-705), a novel viral RNA polymerase inhibitor. *Antiviral Res.* **2013**, *100*, 446-454, <https://doi.org/10.1016/j.antiviral.2013.09.015>.
34. Tu, Y.F.; Chien, C.S.; Yarmishyn, A.A.; Lin, Y.Y.; Luo, Y.H.; Lin, Y.T.; Lai, W.Y.; Yang, D.M.; Chou, S.J.; Yang, Y.P.; Wang, M.L.; Chiou, S.H. A review of SARS-CoV-2 and the ongoing clinical trials. *Int. J. Mol. Sci.* **2020**, *21*, 2657; <https://doi.org/10.3390/ijms21072657>.

Supplementary files

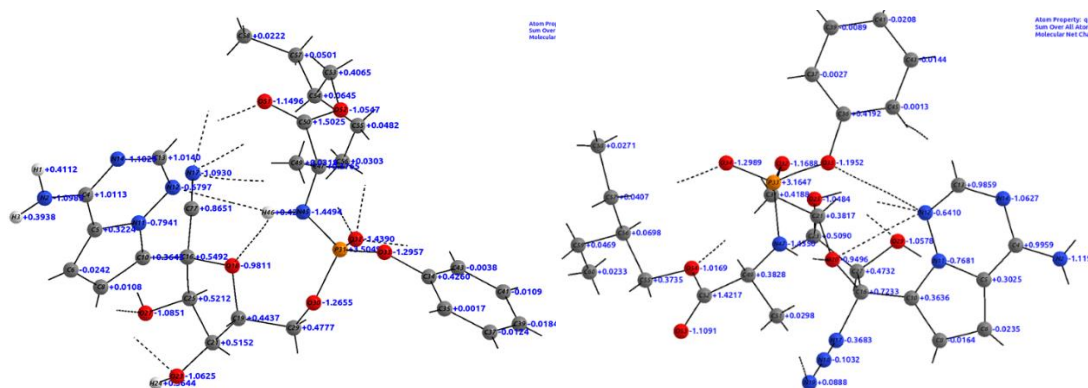
**Table 5.** Atomic charges (qA) of the drugs calculated by AIMAll program.

Remdesivir		AZCV	(S)-Chloroquin	(R)-Chloroquin			
H1	+0.411225	H1	+0.421969	C1	+0.461044	C1	+0.461415
N2	-1.098884	N2	-1.119322	C2	+0.045888	C2	+0.045807
H3	+0.393823	H3	+0.405365	H3	+0.069051	H3	+0.069023
C4	+1.011324	C4	+0.995908	C4	+0.018848	C4	+0.018641
C5	+0.322375	C5	+0.302524	C15	-0.225872	C15	-0.226026
C6	-0.024202	C6	-0.023542	C6	+0.027001	C6	+0.027137
H7	+0.034701	H7	+0.036790	H7	+0.039492	H7	+0.039237
C8	+0.010835	C8	-0.016371	C8	-0.001698	C8	-0.002122
H9	+0.075685	H9	+0.057211	H9	-0.006609	H9	-0.008327
C10	+0.364274	C10	+0.363554	C10	-0.012161	C10	-0.013538
N11	-0.794121	N11	-0.768103	C11	+0.437336	C11	+0.434308
N12	-0.679685	N12	-0.640966	N12	-1.119540	N12	-1.114375
C13	+1.013952	C13	+0.985861	H13	+0.371065	H13	+0.370431
N14	-1.102879	N14	-1.062734	C14	+0.384095	C14	+0.379545
H15	+0.117514	H15	+0.083601	H15	-0.002028	C15	+0.037440
C16	+0.549161	C16	+0.723333	C16	+0.036676	H16	-0.002359
N17	-1.093003	N17	-0.368276	H17	-0.007638	H17	-0.009023
O18	-0.981127	N18	-0.103163	H18	-0.023030	H18	-0.001682
C19	+0.443691	N19	+0.088763	C19	+0.390868	H19	-0.009772
H20	+0.057873	O20	-0.949603	H20	-0.017074	C20	+0.038723
C21	+0.515164	C21	+0.381683	N21	-1.010373	H21	-0.022795
H22	+0.013659	H22	+0.088754	C22	+0.388759	H22	-0.005231
O23	-1.062498	C23	+0.508997	H23	-0.013797	C23	+0.395466
H24	+0.564371	H24	+0.036566	H24	-0.033690	H24	-0.016195
C25	+0.521242	O25	-1.048404	C25	+0.042544	N25	-1.013604
H26	+0.039548	H26	+0.574467	H26	-0.006233	C26	+0.389934
O27	-1.085115	C27	+0.473187	H27	-0.018266	H27	-0.014632
H28	+0.571073	H28	+0.050849	H28	-0.014503	H28	-0.034541
C29	+0.477720	O29	-1.057835	C29	+0.383785	C29	+0.042562
O30	-1.265490	H30	+0.562376	H30	-0.033307	H30	-0.006216
P31	+3.504933	C31	+0.418820	C31	+0.043694	H31	-0.017296
O32	-1.438955	O32	-1.168826	H32	-0.020486	H32	-0.015299
O33	-1.295725	P33	+3.164749	H33	-0.018315	C33	+0.383336
C34	+0.426005	O34	-1.298919	H34	-0.006052	H34	-0.030129
C35	+0.001730	O35	-1.195171	H35	-0.009889	C35	+0.043602
H36	+0.044113	C36	+0.419190	H36	-0.015939	H36	-0.020223
C37	-0.012417	C37	-0.002698	C37	+0.035178	H37	-0.017453
H38	+0.022523	H38	+0.066662	H38	+0.001753	H38	-0.006845
C39	-0.018445	C39	-0.008876	H39	-0.014673	H39	-0.009782
H40	+0.019669	H40	+0.024284	H40	+0.002992	H40	-0.016318
C41	-0.010941	C41	-0.020775	C41	-0.033436	C41	-0.027659
H42	+0.024392	H42	+0.017591	H42	+0.004298	H42	+0.006603
C43	-0.003751	C43	-0.014377	C43	+0.602826	C43	+0.602208
H44	+0.081783	H44	+0.020999	H44	+0.020546	H44	+0.020085
N45	-1.449439	C45	-0.001278	N45	-1.143453	N45	-1.144419
H46	+0.427360	H46	+0.041833				
C47	+0.376478	N47	-1.435039				
H48	+0.057715	H48	+0.438691				
C49	+0.031795	C49	+0.382750				
C50	+1.502472	H50	+0.079239				
O51	-1.149587	C51	+0.029762				
O52	-1.054660	C52	+1.421671				
C53	+0.406467	O53	-1.109101				
C54	+0.064537	O54	-1.016875				
C55	+0.048202	C55	+0.373534				
C56	+0.030275	C56	+0.069803				
C57	+0.050119	C57	+0.040736				
C58	+0.022228	C58	+0.027062				
H59	+0.066577	C59	+0.046918				
H60	+0.039030	C60	+0.023339				
H61	+0.018106	H61	+0.076529				
H62	+0.050762	H62	+0.060796				
H63	+0.009209	H63	+0.058126				

H64	-0.037222	H64	+0.022609
H65	+0.023253	H65	-0.020971
H66	-0.011798	H66	-0.025126
H67	-0.032155	H67	+0.038229
H68	-0.014704	H68	-0.007367
H69	-0.025980	H69	-0.018034
H70	+0.005410	H70	+0.000888
H71	+0.002743	H71	-0.023224
H72	+0.015269	H72	-0.011767
H73	+0.014357	H73	+0.039203
H74	-0.016989	H74	+0.011641
H75	-0.016922	H75	+0.012440
H76	+0.016000	H76	-0.004322
C77	+0.865066	H77	-0.017154
		H78	-0.011716

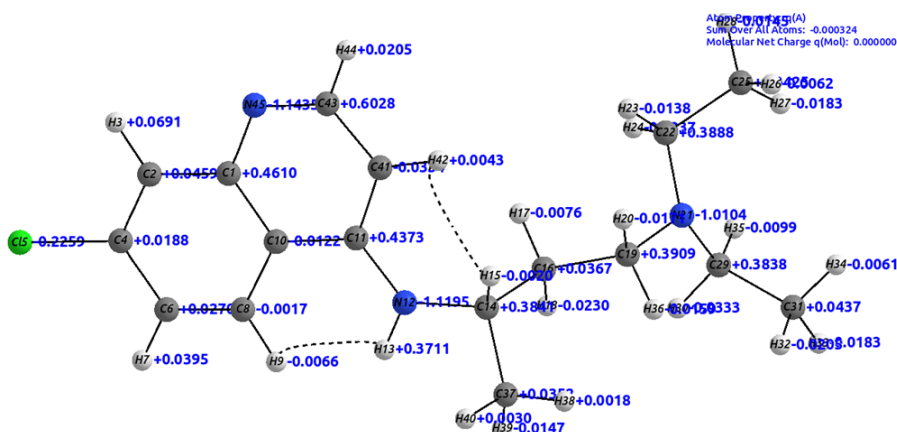
(S)-Hydroxychloroquine		(R)-Hydroxychloroquine		Umifenovir		Favipiravir	
C1	+0.461238	C1	+0.461238	H1	+0.040271	H1	+0.080523
C2	+0.046092	C2	+0.046092	C2	+0.019204	C2	+0.574902
H3	+0.069546	H3	+0.069546	C3	-0.082892	N3	-1.122517
C4	+0.019018	C4	+0.019018	C4	+0.569945	C4	+1.091433
C15	-0.224697	C15	-0.224697	O5	-1.139220	O5	-1.068268
C6	+0.027113	C6	+0.027113	H6	+0.602150	H6	+0.585338
H7	+0.039822	H7	+0.039822	C7	-0.005783	C7	+0.509856
C8	-0.002185	C8	-0.002185	C8	+0.317457	C8	+1.448474
H9	-0.008443	H9	-0.008443	N9	-0.972799	N9	-1.132115
C10	-0.013382	C10	-0.013382	C10	+0.332807	H10	+0.409469
C11	+0.432877	C11	+0.432877	H11	+0.013826	H11	+0.426064
N12	-1.114451	N12	-1.114451	H12	+0.010450	O12	-1.117988
H13	+0.370882	H13	+0.370882	H13	-0.009927	N13	-1.143699
C14	+0.382023	C14	+0.382023	C14	+0.321095	C14	+1.072602
C15	+0.036616	C15	+0.036616	H15	+0.025624	F15	-0.614027
H16	-0.001393	H16	-0.001393	H16	-0.013319		
H17	-0.007722	H17	-0.007722	H17	+0.010627		
H18	-0.000511	H18	-0.000511	H18	+0.032689		
H19	-0.008868	H19	-0.008868	H19	+0.031312		
C20	+0.037999	C20	+0.037999	C20	+0.001441		
H21	-0.021574	H21	-0.021574	C21	-0.014326		
H22	-0.003612	H22	-0.003612	C22	+1.471940		
C23	+0.378038	C23	+0.378038	O23	-1.055553		
H24	-0.008416	H24	-0.008416	C24	+0.441061		
N25	-1.001253	N25	-1.001253	C25	+0.029985		
C26	+0.357123	C26	+0.357123	H26	+0.028884		
H27	+0.000312	H27	+0.000312	H27	+0.000596		
H28	-0.023390	H28	-0.023390	H28	+0.001218		
C29	+0.520765	C29	+0.520765	H29	+0.045557		
O30	-1.088719	O30	-1.088719	H30	+0.019380		
H31	+0.561904	H31	+0.561904	O31	-1.155849		
H32	-0.016636	H32	-0.016636	C32	+0.409271		
H33	+0.011908	H33	+0.011908	N33	-1.164363		
C34	+0.369942	C34	+0.369942	C34	+0.357820		
H35	-0.031274	H35	-0.031274	H35	+0.033289		
C36	+0.042419	C36	+0.042419	H36	+0.030073		
H37	-0.019460	H37	-0.019460	H37	+0.038496		
H38	-0.004433	H38	-0.004433	C38	+0.359562		
H39	-0.003583	H39	-0.003583	C39	-0.044002		
H40	-0.007283	H40	-0.007283	S40	+0.003765		
H41	-0.011966	H41	-0.011966	C41	-0.126515		
C42	-0.028139	C42	-0.028139	C42	-0.004218		
H43	+0.005714	H43	+0.005714	H43	+0.032937		

C44	+0.603329	C44	+0.603329	C44	-0.014255
H45	+0.020624	H45	+0.020624	H45	+0.022119
N46	-1.143917	N46	-1.143917	C46	-0.014563
				H47	+0.023410
				C48	-0.007106
				H49	+0.030860
				C50	+0.002260
				H51	+0.041445
				H52	+0.036000
				H53	+0.096258
				Br54	-0.059462

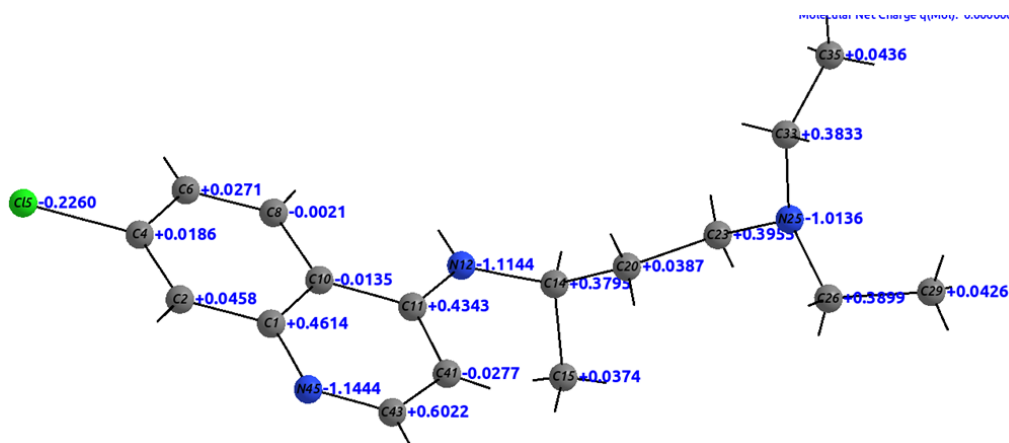


Remdesevir

AZCV-20



(R)-Chloroquine



(S)-Chloroquine

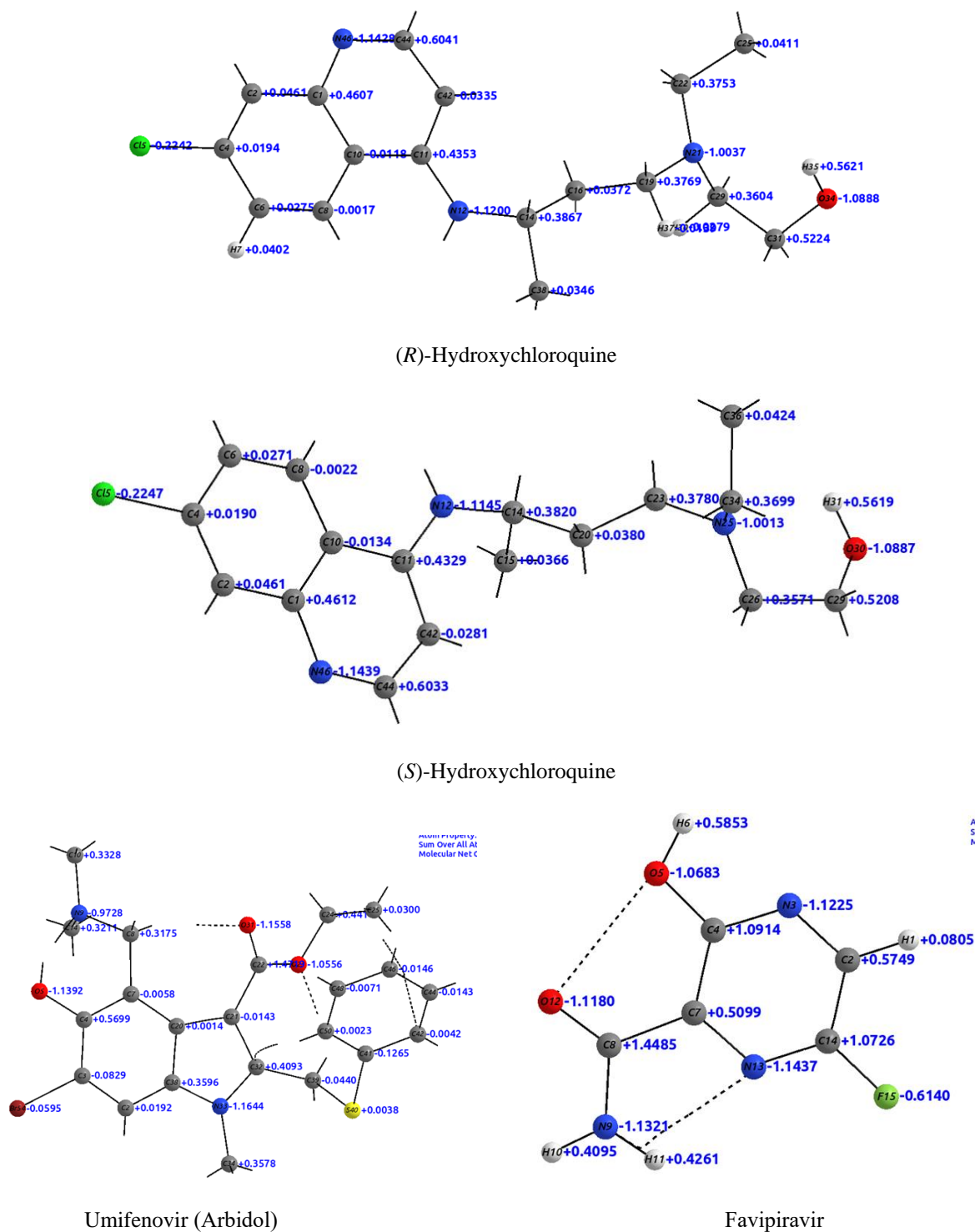


**Figure 4.** Atomic charges (qA) calculated by AIMAll program (according to Bader Atoms-in-Molecules theory)